Eur. Phys. J. B **32**, 27–33 (2003)
DOI: 10.1140/epjb/e2003-00070-2

THE EUROPEAN PHYSICAL JOURNAL B

A theoretical analysis of the magnetic properties of La_2CuO_4

A. Avella[a] and F. Mancini

Dipartimento di Fisica "E.R. Caianiello" - Unità di ricerca INFM di Salerno, Università degli Studi di Salerno, 84081 Baronissi (SA), Italy

Received 29 July 2002 / Received in final form 2 January 2003
Published online 14 March 2003 –

Abstract. The magnetic properties of the La_2CuO_4 are analyzed by means of the paramagnetic solution of the Hubbard model within the composite operator method. The experimental findings of the inelastic neutron magnetic scattering [R. Coldea *et al.*, Phys. Rev. Lett. **86**, 5377 (2001)] for the spin spectrum, the spin-wave intensity and the behavior of the dispersion at the zone boundary are well described by our results although the difference in phase. The Hubbard model emerges has a minimal model capable to describe the anomalous magnetic behavior of such a strongly correlated material.

PACS. 75.50.-y Studies of specific magnetic materials – 71.10.-w Theories and models of many-electron systems – 71.27.+a Strongly correlated electron systems; heavy fermions

1 Introduction

There is a spread wide consensus that some high temperature cuprate superconductors, in particular the LSCO family, are well described by the t-J model, which reduces to the Heisenberg model at half-filling. A recent experiment [1] casts some doubts on this belief. By using inelastic neutron scattering as a probe to analyze magnetic excitations in the parent compound La_2CuO_4, it has been shown that nearest-neighbor interactions among the Cu^{2+} spins are not sufficient to explain the experimental behavior. Along the antiferromagnetic boundary of the Brillouin zone the spin wave energy is not constant, as predicted [2] by the spin wave theory of the nearest-neighbor Heisenberg model, but exhibits a noticeable dispersion. By introducing wave-vector-dependent quantum corrections to the spin-wave energies, a dispersion along the zone boundary has been obtained [3–6], but with an opposite sign to the experimental results of reference [1]. As shown in reference [1], in order to describe the observed dispersion relation one needs to generalize [7–11] the Heisenberg model by introducing higher-order couplings: J' and J'', which describe second- and third-nearest neighbor interactions, respectively; J_c which describes ring exchange interactions coupling four spins at the corners of the CuO_4 square plaquette. On the other hand, as noticed by the authors of reference [1], these higher-order interactions are naturally present in the single-band Hubbard model. This is due to the electron hopping among the Cu sites which induces charge fluctuations with finite double occupancy and can be explicitly seen by expanding the Hubbard Hamiltonian up to the t^4/U^3-order. As shown in references [7–9,11], one obtains $J' = J'' = 4t^4/U^3$ and $J_c = 80t^4/U^3$. The same result is not true for the t-J model, where only the first-nearest neighbor coupling $J = 4t^2/U$ is taken into account. As matter of fact, a two-pole approximation of the two-dimensional Hubbard model, in the context of the composite operator method (COM) [12–16], yields [17] a double occupancy at $n = 1$ and $T = 0$ that in the limit $U \gg t$ goes as $D = 2\frac{t^2}{U^2} + O(\frac{t^4}{U^4})$ showing that there always exists a finite double occupancy for any value of the Coulomb repulsion U which reduces the number of spins involved in the magnetic response.

The fact that first-nearest neighbor spin interactions are not sufficient to describe the experimental situations has also been reported in other circumstances: Raman scattering, infrared absorption, $Sr_2CuO_2Cl_2$ [18], $Sr_{14}Cu_{24}O_{41}$ compound (see Ref. [1] for discussion and related references).

Summarizing, there is experimental evidence that in some highly correlated systems the electronic excitations induce magnetic interactions beyond the nearest-neighbor term. The Heisenberg and t-J models are not sufficient and a minimal model which contains higher-order terms can be given by the Hubbard model.

2 The bosonic sector of the Hubbard model

In this work, we analyze the magnetic properties of the Hubbard model in the paramagnetic phase. These properties are described by two-particle Green's functions (2PGF) and to compute them there exist mainly two approaches. The first one is to expand the 2PGF in terms of the single-particle propagators. The second one is to

[a] e-mail: avella@sa.infn.it

calculate directly the 2PGF by means of the equations of motion. Both approaches require some approximation. In the first case, one can choose to use the diagrammatic expansion of the RPA and compute the fermionic lines (*i.e.*, the electronic Green's functions) in the mean field approximation [19]; a different approximation scheme is based on the use of the Hubbard propagators as building blocks of the fermionic loops [14,15]. Here, we will follow the second approach, that based on the equations of motion, in the framework of the composite operator method.

The two-dimensional single-band Hubbard model is described by the following Hamiltonian

$$H = \sum_{\mathbf{ij}} \big[-4t\,\alpha_{\mathbf{ij}}\, c^\dagger(\mathbf{i})\, c(\mathbf{j}) - \mu\,\delta_{\mathbf{ij}}\, c^\dagger(\mathbf{i})\, c(\mathbf{j}) + U\,\delta_{\mathbf{ij}}\, n_\uparrow(\mathbf{i})\, n_\downarrow(\mathbf{j}) \big]. \quad (1)$$

The notation is the following. $c^\dagger(i) = (c^\dagger_\uparrow(i), c^\dagger_\downarrow(i))$ is the electron creation operator in spinorial notation at the site $\mathbf{i}$ [$i = (\mathbf{i}, t)$] and $n_\sigma(i) = c^\dagger_\sigma(i)\, c_\sigma(i)$ is the number operator for spin σ at the site $\mathbf{i}$; t is the transfer integral, μ is the chemical potential and U is the on-site Coulomb repulsion, $\alpha_{\mathbf{ij}}$ is the projector operator on the first-nearest-neighbor sites (see Appendix). Hereafter, for a generic operator $\zeta(i)$, we will use the notation $\zeta^\alpha(i)$ to indicate its projection on the first-nearest-neighbor sites (see Appendix).

Let us introduce the composite bosonic field [20]

$$N_\nu(i) = \begin{pmatrix} n_\nu(i) \\ \rho_\nu(i) \end{pmatrix} \quad (2)$$

where

$$n_\nu(i) = c^\dagger(i)\,\sigma_\nu\, c(i) \quad (3)$$

$$\rho_\nu(i) = c^\dagger(i)\,\sigma_\nu\, c^\alpha(i) - c^{\dagger\alpha}(i)\,\sigma_\nu\, c(i). \quad (4)$$

We note that $n_\nu(i)$ is the charge ($\nu = 0$) and spin ($\nu = 1,2,3$) density operator, with $\sigma_\nu = (1, \boldsymbol{\sigma})$, $\sigma^\nu = (-1, \boldsymbol{\sigma})$ and $\boldsymbol{\sigma}$ are the Pauli matrices. The composite field $N_\nu(i)$ satisfies the Heisenberg equation

$$\mathrm{i}\frac{\partial}{\partial t} N_\nu(i) = J_\nu(i) = \begin{pmatrix} -4t\,\rho_\nu(i) \\ -4t\, l_\nu(i) + U\,\kappa_\nu(i) \end{pmatrix} \quad (5)$$

with

$$\kappa_\nu(i) = c^\dagger(i)\,\sigma_\nu\,\eta^\alpha(i) - \eta^\dagger(i)\,\sigma_\nu\, c^\alpha(i) + \eta^{\dagger\alpha}(i)\,\sigma_\nu\, c(i) - c^{\dagger\alpha}(i)\,\sigma_\nu\,\eta(i) \quad (6)$$

$$l_\nu(i) = c^\dagger(i)\,\sigma_\nu\, c^{\alpha^2}(i) + c^{\dagger\alpha^2}(i)\,\sigma_\nu\, c(i) - 2c^{\dagger\alpha}(i)\,\sigma_\nu\, c^\alpha(i). \quad (7)$$

We linearize the equation of motion (5) by projecting the source $J_\nu(i)$ on the basis $N_\nu(i)$ and obtain

$$\mathrm{i}\frac{\partial}{\partial t} N_\nu(\mathbf{i}, t) \cong \sum_{\mathbf{j}} \varepsilon^{(\nu)}(\mathbf{i}, \mathbf{j})\, N_\nu(\mathbf{j}, t). \quad (8)$$

In the paramagnetic phase, $\varepsilon^{(\nu)}(\mathbf{k})$, the Fourier transform of the energy matrix $\varepsilon^{(\nu)}(\mathbf{i}, \mathbf{j})$, reads as

$$\varepsilon^{(\nu)}(\mathbf{k}) = m^{(\nu)}(\mathbf{k}) \left[I^{(\nu)}(\mathbf{k}) \right]^{-1} \quad (9)$$

where

$$I^{(\nu)}(\mathbf{k}) = \mathcal{F} \left\langle \left[N_\nu(\mathbf{i}, t), N^\dagger_\nu(\mathbf{j}, t) \right] \right\rangle \quad (10)$$

$$m^{(\nu)}(\mathbf{k}) = \mathcal{F} \left\langle \left[J_\nu(\mathbf{i}, t), N^\dagger_\nu(\mathbf{j}, t) \right] \right\rangle \quad (11)$$

$\langle \cdots \rangle$ indicates the thermal average in the grand canonical ensemble and the symbol $\mathcal{F}$ denotes the Fourier transform. Let us consider the causal thermal Green's function

$$G^{(\nu)}(i, j) = \left\langle T \left[N_\nu(i)\, N^\dagger_\nu(j) \right] \right\rangle \quad (12)$$

and the correlation function

$$C^{(\nu)}(i, j) = \left\langle N_\nu(i)\; N^\dagger_\nu(j) \right\rangle . \quad (13)$$

By means of the equation of motion (8), the Fourier transforms of these quantities satisfy the following equations

$$\left[\omega - \varepsilon^{(\nu)}(\mathbf{k}) \right] G^{(\nu)}(\mathbf{k}, \omega) = I^{(\nu)}(\mathbf{k}) \quad (14)$$

$$\left[\omega - \varepsilon^{(\nu)}(\mathbf{k}) \right] C^{(\nu)}(\mathbf{k}, \omega) = 0. \quad (15)$$

The solution of these equations gives [21]

$$G^{(\nu)}(\mathbf{k}, \omega) = -\mathrm{i}\frac{(2\pi)^3}{a^2}\delta^{(2)}(\mathbf{k})\,\delta(\omega)\,\Gamma_\nu + \sum_{n=1}^{2} \sigma^{(n,\nu)}(\mathbf{k}) \times \left[\frac{1 + f_{\mathrm{B}}(\omega)}{\omega - \omega^{(\nu)}_n(\mathbf{k}) + \mathrm{i}\,\delta} - \frac{f_{\mathrm{B}}(\omega)}{\omega - \omega^{(\nu)}_n(\mathbf{k}) - \mathrm{i}\,\delta} \right] \quad (16)$$

$$C^{(\nu)}(\mathbf{k}, \omega) = \frac{(2\pi)^3}{a^2}\delta^{(2)}(\mathbf{k})\,\delta(\omega)\,\Gamma_\nu + 2\pi \sum_{n=1}^{2} \delta \left[\omega - \omega^{(\nu)}_n(\mathbf{k}) \right] \left[1 + f_{\mathrm{B}}(\omega) \right] \sigma^{(n,\nu)}(\mathbf{k}) \quad (17)$$

where a is the lattice constant, which will be set 1 hereafter, and $f_{\mathrm{B}}(\omega) = \frac{1}{\mathrm{e}^{\beta\omega} - 1}$ is the Bose function. The energy spectra and the spectral density functions have the expressions

$$\omega^{(\nu)}_n(\mathbf{k}) = (-)^n\, \omega^{(\nu)}(\mathbf{k}) \quad (18)$$

$$\omega^{(\nu)}(\mathbf{k}) = \sqrt{-4t\,\frac{m^{(\nu)}_{22}(\mathbf{k})}{I^{(\nu)}_{12}(\mathbf{k})}} \quad (19)$$

$$\sigma^{(n,\nu)}(\mathbf{k}) = \frac{1}{2} I^{(\nu)}_{12}(\mathbf{k}) \begin{pmatrix} -\frac{4t}{\omega^{(\nu)}_n(\mathbf{k})} & 1 \\ 1 & -\frac{\omega^{(\nu)}_n(\mathbf{k})}{4t} \end{pmatrix} . \quad (20)$$

The explicit expressions of the functions $I^{(\nu)}_{12}(\mathbf{k})$ and $m^{(\nu)}_{22}(\mathbf{k})$ are reported in Appendix. The matrix Γ_ν is the

zero frequency constant; as discussed in reference [21], this function is not determined by the equations of motion or by the boundary conditions and must be calculated by other means. The charge and spin equal-time correlation functions are given by

$$\langle n_\nu(\mathbf{i})\, n_\nu(\mathbf{j})\rangle = \Gamma_{11\nu} - \frac{2t}{(2\pi)^2}\int_{\Omega_{\rm B}} \mathrm{d}\mathbf{k}\, \mathrm{e}^{\mathrm{i}\,\mathbf{k}(\mathbf{i}-\mathbf{j})}\frac{I_{12}^{(\nu)}(\mathbf{k})}{\omega^{(\nu)}(\mathbf{k})}\coth\frac{\beta\,\omega^{(\nu)}(\mathbf{k})}{2} \quad (21)$$

where $\Omega_{\rm B}$ is the volume of the unit cell in the reciprocal space.

Within the linear response theory, the charge and spin susceptibilities are given by the opposite of the retarded thermal Green's function

$$\chi^{(\nu)}(\mathbf{k},\omega) = -\mathcal{F}\,\langle R\,[n_\nu(i)\, n_\nu(j)]\rangle = -\sum_{n=1}^{2}\frac{\sigma_{11}^{(n,\nu)}(\mathbf{k})}{\omega-\omega_n^{(\nu)}(\mathbf{k})+\mathrm{i}\,\delta}\,. \quad (22)$$

In particular, the static susceptibilities have the expression

$$\chi^{(\nu)}(\mathbf{k}) = \frac{\left[I_{12}^{(\nu)}(\mathbf{k})\right]^2}{m_{22}^{(\nu)}(\mathbf{k})}\,. \quad (23)$$

All these expressions are only formal because depend on a set of parameters which have to be calculated. In particular, we can distinguish: (i) external parameters: n, T, U; (ii) fermionic correlators: C^α, C^λ, C^ϖ, D, E^β, E^η; (iii) bosonic correlators: a_ν, b_ν, c_ν, d_ν; (iv) zero-frequency constants: $\Gamma_{11\nu}$. All these parameters are defined in Appendix where you can also find the relations in which they appear in connection with the physical quantities analyzed so far.

The fermionic correlators can be calculated according to the scheme given in references [12–16], where the fermionic sector of the Hubbard model has been solved in the framework of the COM in the two-pole approximation. In order to fix the bosonic parameters we use the following procedure. The condition that the static susceptibilities $\chi^{(\nu)}(\mathbf{0})$ are finite single-value functions gives the following expressions for the parameters b_ν, c_ν and d_ν

$$b_\nu = a_\nu + 3D + E^\eta + 2E^\beta - 6\frac{t}{U}\left(C^\alpha + C^\lambda - 2C^\varpi\right) \quad (24)$$

$$c_\nu = a_\nu - D + E^\eta - 2E^\beta + 6\frac{t}{U}\left(C^\alpha + C^\lambda - 2C^\varpi\right) \quad (25)$$

$$d_\nu = a_\nu - D - 3E^\eta + 2E^\beta - 6\frac{t}{U}\left(C^\alpha + C^\lambda - 2C^\varpi\right). \quad (26)$$

The remaining bosonic correlators a_ν are determined by means of the Pauli principle which requires

$$\langle n(i)\, n(i)\rangle = n + 2D \quad (27a)$$

$$\langle n_k(i)\, n_k(i)\rangle = n - 2D \qquad k = 1,\ 2,\ 3. \quad (27b)$$

Finally, the zero frequency constants are fixed by setting the ergodic values: $\Gamma_{11\nu} = \delta_{\nu 0}\, n^2$.

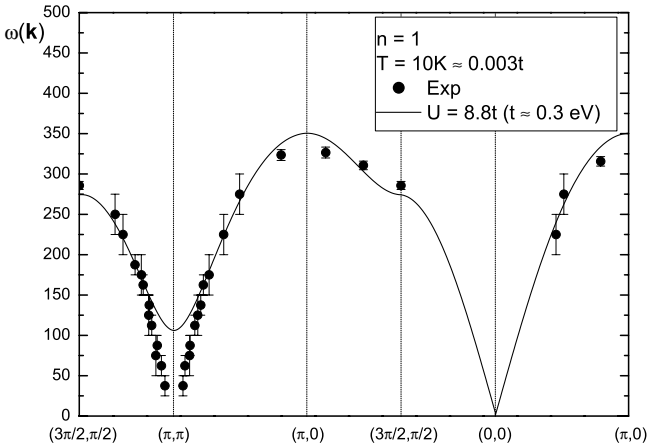

Fig. 1. The energy spectrum $\omega^{(3)}(\mathbf{k})$ of the spin propagator along the principal directions for $n = 1$, $T = 10$ K and $U = 8.8t$. The experimental data are taken from reference [1].

Once the external parameters have been set, the analysis will follow these steps: 1) we solve the fermionic sector and obtain the relative correlators as in references [12–16]; 2) we solve the self-consistent equations for a_ν and obtain the bosonic propagators; 3) we compute the response functions (the susceptibilities) from the causal bosonic Green's functions.

3 Results

In Figure 1, we report the energy spectrum $\omega^{(3)}(\mathbf{k})$ of the spin propagator along the principal directions and compare it with the experimental data of reference [1] obtained for La_2CuO_4 by means of inelastic magnetic neutron scattering. We have chosen the value of the temperature ($T = 10$ K) according to the experimental set-up; the value of the transfer integral ($t = 0.3$ eV) and of the Coulomb repulsion ($U = 2.6$ eV) have been chosen in order to fit the experimental points and they are within the ranges ($t = 0.3 \pm 0.02$ eV; $U = 2.2 \pm 0.4$ eV) suggested in reference [1]. The agreement with the experimental data is very good all over the momentum space except around $\mathbf{Q} = (\pi, \pi)$. As a matter of fact, the experimental data refer to the antiferromagnetic phase of the material (the experimental spectrum gets *soft* at $\mathbf{Q}$ and, obviously, our paramagnetic solution cannot fully describe such behavior). However, it is worth noting that the Hubbard model at half-filling present so strong antiferromagnetic correlations that they also show up in the paramagnetic phase through a quite pronounced minimum at $\mathbf{Q}$. Very good results have been also obtained within a dressed RPA resolved in the antiferromagnetic phase by Peres *et al.* [19].

The spin-wave intensity, calculated within the present approach, is reported in Figure 2 and compared with the experimental data of reference [1]. The agreement is again very good over all the momentum space and shows once more the capability of the Hubbard model, within our formulation, to catch the physics of such a strongly correlated system.

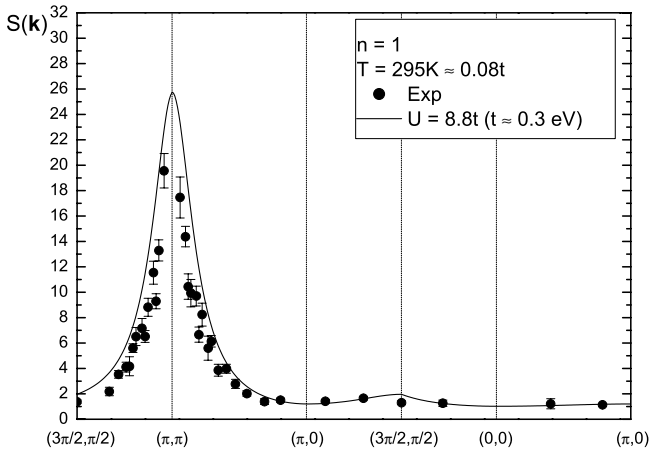

Fig. 2. The spin-wave intensity along the principal directions for $n = 1$, $T = 295$ K and $U = 8.8t$. The experimental data are taken from reference [1].

In order to get a deeper comprehension of the tendency towards an antiferromagnetic ordering, clearly shown by our results (we reported a quite pronounced minimum in the spin spectrum and a very large peak in the spin-wave intensity, both at $\mathbf{Q}$), we have computed the antiferromagnetic correlation length ξ, within our approach, by expanding in series the static susceptibility (23) around $\mathbf{k} = \mathbf{Q}$. We have obtained

$$\chi^{(3)}(\mathbf{k}) = \frac{\chi^{(3)}(\mathbf{Q})}{1 + \xi^2 \left|\mathbf{k} - \mathbf{Q}\right|^2} + O\left(\left|\mathbf{k} - \mathbf{Q}\right|^4\right). \qquad (28)$$

Explicit calculations showed that, within our approach, the antiferromagnetic correlation length ξ can be cast in the following form

$$\xi^2 = \frac{1}{8}\left(\frac{\chi^{(3)}(\mathbf{Q})}{\chi^{(3)}(\mathbf{0})} - 1\right). \qquad (29)$$

In Figures 3 and 4, we report the antiferromagnetic correlation length ξ and the value of the energy spectrum of the spin propagator at $\mathbf{Q}$, $\omega^{(3)}(\mathbf{Q})$, as functions of temperature and Coulomb repulsion, respectively. As expectable, it is evident the enhancement of the antiferromagnetic correlation length ξ on lowering the temperature and on increasing the Coulomb repulsion. As a matter of fact, a large value of the Coulomb repulsion U (larger than $U \approx 9$) results counterproductive as reduces the value of the exchange integral J. This latter results fully effective, within the paramagnetic phase, only in the intermediate-strong coupling regime, where the expansion in t/U begins to be applicable and the resulting value $J = 4t^2/U$ is not too small. As regards the energy spectrum of the spin propagator at $\mathbf{Q}$, $\omega^{(3)}(\mathbf{Q})$, we report a behavior just the opposite to that of ξ on the whole ranges of temperature and potential strength. After this analysis we can conclude that although a very strong tendency towards an antiferromagnetic ordering can be recognized in the behavior of all reported quantities, the finite value of $\omega^{(3)}(\mathbf{Q})$ at $T = 0$ for any finite value of the Coulomb repulsion U shows the

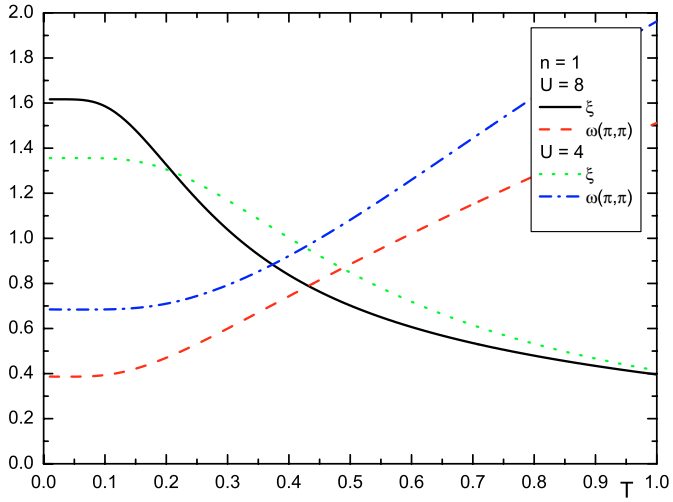

Fig. 3. The antiferromagnetic correlation length ξ and the value of the energy spectrum of the spin propagator at $\mathbf{Q}$, $\omega^{(3)}(\mathbf{Q})$, as functions of the temperature T for $n = 1$ and $U = 4t$ and $8t$.

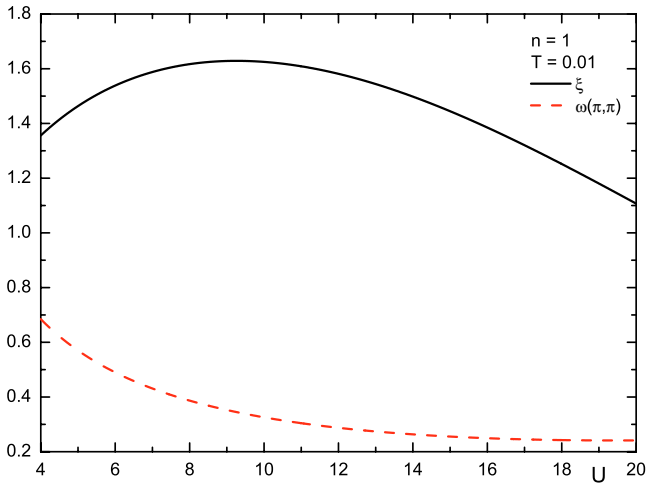

Fig. 4. The antiferromagnetic correlation length ξ and the value of the energy spectrum of the spin propagator at $\mathbf{Q}$, $\omega^{(3)}(\mathbf{Q})$, as functions of the Coulomb repulsion U for $n = 1$ and $T = 0.01t$.

absence of an antiferromagnetic instability at half filling in our paramagnetic solution. This could be due to the lack of self-energy corrections in the present formulation. At any rate, it is worth noticing that we reported a very rich antiferromagnetic solution for the fermionic sector of the Hubbard model within our formulation in reference [16], but the complexity of the calculations have not permitted yet the extension of such solution to the bosonic sector.

Coming back to our comparison with the experimental results of reference [1], we can estimate the zone-boundary spin-wave dispersion through the quantity

$$\varkappa(U,T) = 2\frac{\omega(\pi,0) - \omega(3\pi/2,\pi/2)}{\omega(\pi,0) + \omega(3\pi/2,\pi/2)}. \qquad (30)$$

In Figure 5 we plot $\varkappa$ as a function of T for $U = 8.8t$. We see that the dispersion decreases as T increases in

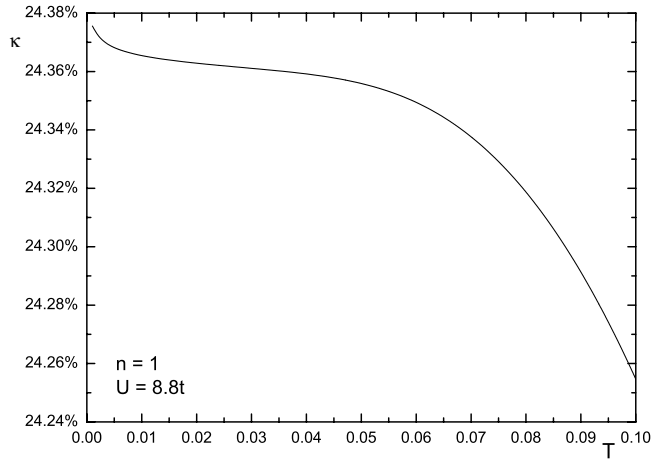

Fig. 5. $\varkappa$, definition in the text, as a function of the temperature T for $n = 1$ and $U = 8.8t$.

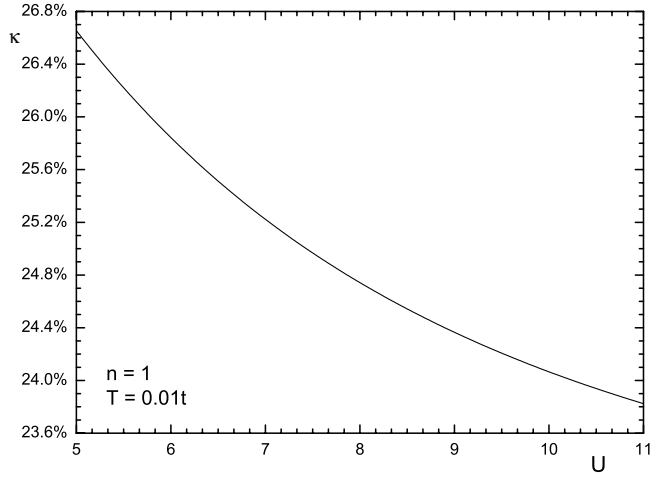

Fig. 6. $\varkappa$, definition in the text, as a function of the Coulomb repulsion U for $n = 1$ and $T = 0.01t$.

agreement with the experimental data. Actually, in reference [1], a much bigger variation in temperature is reported. The quantitative discrepancy can be understood as a consequence of the difference in phase existing between the analytical and the experimental data. Within the antiferromagnetic phase, which is the one experimentally observed, the dispersion at the zone boundary is very sensitive to the competition between the low energy scale J and the temperature T. Our data, computed within the paramagnetic phase, are very much less sensitive to it. $\varkappa$ as a function of U for $T = 0.01t$ is reported in Figure 6. The dispersion is also reduced on increasing the Coulomb repulsion and goes to zero only for U infinity. This result is in agreement with the behavior known for the simple t-J model, which is the strong coupling limit of the Hubbard model. In fact, the simple t-J model, by the absence of the extended exchange couplings which vanish as t^4/U^4, does not present any dispersion along the zone boundary. The experimental data show such dispersion and consequently suggest an intermediate-strong coupling regime which result inaccessible to the simple t-J model.

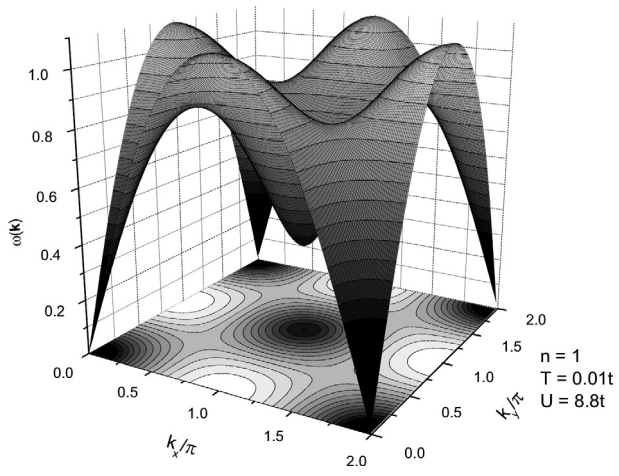

Fig. 7. The energy spectrum $\omega^{(3)}(\mathbf{k})$ of the spin propagator for $n = 1$, $T = 0.01t$ and $U = 8.8t$.

Finally, in Figure 7 we show the spin spectrum on the entire Brillouin zone for the same values of the external parameters. The picture clearly shows the correct behavior at $(0, 0)$, the minimum at $\mathbf{Q}$ and the dispersion along the zone boundary.

4 Conclusions

In conclusion, we have studied the magnetic properties of the La_2CuO_4 by means of the paramagnetic solution of the Hubbard model within the composite operator method. The experimental findings of the inelastic neutron magnetic scattering [1] for the spin spectrum, the spin-wave intensity and the behavior of the dispersion at the zone boundary are very well described by our results and confirm the idea, which is also suggested by many recent publications, both theoretical and experimental, that the cuprates fall in the intermediate-strong coupling regime. This regime cannot be properly described by the simple t-J model, which is derived from the Hubbard model in the strong coupling regime. Extended exchange couplings, dynamically generated in the Hubbard model at the higher order of the expansion in t/U, seem relevant to describe all the experimental features of the dispersion. The Hubbard Hamiltonian results still as the best candidate to catch the physical behavior of these materials.

We wish to thank S.-W. Cheong, G. Aeppli and R. Coldea for providing us with the experimental data [1].

Appendix

For a generic operator $\zeta(i)$, we use the notation $\zeta^\alpha(i)$ to indicate the projection on the first-nearest-neighbor sites

$$\zeta^\alpha(\mathbf{i}, t) = \sum_{\mathbf{j}} \alpha_{\mathbf{ij}}\, \zeta(\mathbf{j}, t) \tag{31}$$

$\alpha_{\mathbf{ij}}$ being the projector operator:

$$\alpha_{\mathbf{ij}} = \frac{1}{N}\sum_{\mathbf{k}} \mathrm{e}^{\mathrm{i}\,\mathbf{k}(\mathbf{i}-\mathbf{j})}\alpha(\mathbf{k}) \tag{32}$$

$$\alpha(\mathbf{k}) = \frac{1}{2}\left[\cos\left(k_x\,a\right) + \cos\left(k_y\,a\right)\right]. \tag{33}$$

The notation $\zeta^{\alpha^2}(i)$ stands for

$$\begin{aligned}\zeta^{\alpha^2}(\mathbf{i},t) &= \sum_{\mathbf{jl}} \alpha_{\mathbf{ij}}\,\alpha_{\mathbf{jl}}\,\zeta\left(\mathbf{l},t\right)\\ &= \frac{1}{4}\left[\zeta(\mathbf{i},t) + 2\zeta^{\beta}\left(\mathbf{i},t\right) + \zeta^{\eta}(\mathbf{i},t)\right]\end{aligned} \tag{34}$$

where by $\zeta^{\beta}(\mathbf{i},t)$ and $\zeta^{\eta}(\mathbf{i},t)$, we denote the projection on the second-nearest-neighbor sites:

$$\beta_{\mathbf{ij}} = \frac{1}{N}\sum_{\mathbf{k}} \mathrm{e}^{\mathrm{i}\,\mathbf{k}(\mathbf{i}-\mathbf{j})}\beta(\mathbf{k})$$

$$\beta(\mathbf{k}) = \frac{1}{2}\left\{\cos\left[\left(k_x + k_y\right)a\right] + \cos\left[\left(k_x - k_y\right)a\right]\right\} \tag{35}$$

$$\eta_{\mathbf{ij}} = \frac{1}{N}\sum_{\mathbf{k}} \mathrm{e}^{\mathrm{i}\,\mathbf{k}(\mathbf{i}-\mathbf{j})}\eta(\mathbf{k})$$

$$\eta(\mathbf{k}) = \frac{1}{2}\left[\cos\left(2k_x\,a\right) + \cos\left(2k_y\,a\right)\right]. \tag{36}$$

The notation $\zeta^{\alpha^3}(i)$ stands for

$$\begin{aligned}\zeta^{\alpha^3}(\mathbf{i},t) &= \sum_{\mathbf{jlm}} \alpha_{\mathbf{ij}}\,\alpha_{\mathbf{jl}}\,\alpha_{\mathbf{lm}}\,\zeta\left(\mathbf{m},t\right)\\ &= \frac{1}{16}\left[9\zeta^{\alpha}\left(\mathbf{i},t\right) + \zeta^{\lambda}(\mathbf{i},t) + 6\zeta^{\varpi}(\mathbf{i},t)\right]\end{aligned} \tag{37}$$

where by $\zeta^{\varpi}(\mathbf{i},t)$ and $\zeta^{\lambda}(\mathbf{i},t)$, we denote the projection on the third-nearest-neighbor sites:

$$\varpi_{\mathbf{ij}} = \frac{1}{N}\sum_{\mathbf{k}} \mathrm{e}^{\mathrm{i}\,\mathbf{k}(\mathbf{i}-\mathbf{j})}\varpi(\mathbf{k}) \tag{38}$$

$$\begin{aligned}\varpi(\mathbf{k}) = \frac{1}{4}\{&\cos\left[\left(2k_x + k_y\right)a\right] + \cos\left[\left(2k_x - k_y\right)a\right]\\ &+ \cos\left[\left(k_x + 2k_y\right)a\right] + \cos\left[\left(k_x - 2k_y\right)a\right]\}\end{aligned} \tag{39}$$

$$\lambda_{\mathbf{ij}} = \frac{1}{N}\sum_{\mathbf{k}} \mathrm{e}^{\mathrm{i}\,\mathbf{k}(\mathbf{i}-\mathbf{j})}\lambda(\mathbf{k}) \tag{40}$$

$$\lambda(\mathbf{k}) = \frac{1}{2}\left[\cos\left(3k_x\,a\right) + \cos\left(3k_y\,a\right)\right]. \tag{41}$$

As it can be easily verified, in the paramagnetic phase the normalization matrix $I^{(\nu)}$ does not depend on the index ν; charge and spin operators have the same weight. The two matrices $I^{(\nu)}$and $m^{(\nu)}$ have the following form in momentum space

$$I^{(\nu)}(\mathbf{k}) = \begin{pmatrix} 0 & I_{12}^{(\nu)}(\mathbf{k}) \\ I_{12}^{(\nu)}(\mathbf{k}) & 0 \end{pmatrix} \tag{42}$$

$$m^{(\nu)}(\mathbf{k}) = \begin{pmatrix} m_{11}^{(\nu)}(\mathbf{k}) & 0 \\ 0 & m_{22}^{(\nu)}(\mathbf{k}) \end{pmatrix} \tag{43}$$

where

$$I_{12}^{(\nu)}(\mathbf{k}) = 4\left[1-\alpha(\mathbf{k})\right]C^{\alpha} \tag{44}$$

$$m_{11}^{(\nu)}(\mathbf{k}) = -4t\,I_{12}^{(\nu)}(\mathbf{k}) \tag{45}$$

$$m_{22}^{(\nu)}(\mathbf{k}) = -4t\,I_{l_\nu\rho_\nu}(\mathbf{k}) + U\,I_{\kappa_\nu\rho_\nu}(\mathbf{k}) \tag{46}$$

and

$$\begin{aligned}I_{l_\nu\rho_\nu}(\mathbf{k}) = &\frac{3}{4}\left[1-\alpha(\mathbf{k})\right]\left(12C^{\alpha} + C^{\lambda} + 6C^{\varpi}\right)\\ &- \frac{3}{4}\left[1-\eta(\mathbf{k})\right]\left(C^{\alpha} + C^{\lambda} + 2C^{\varpi}\right)\\ &+ \frac{1}{4}\left[1-\lambda(\mathbf{k})\right]C^{\lambda} + \frac{3}{2}\left[1-\varpi(\mathbf{k})\right]C^{\varpi}\\ &- 3\left[1-\beta(\mathbf{k})\right]\left(C^{\alpha} + C^{\varpi}\right)\end{aligned} \tag{47}$$

$$\begin{aligned}I_{\kappa_\nu\rho_\nu}(\mathbf{k}) = &-2\left[1-\alpha(\mathbf{k})\right]D + \left[1-2\alpha(\mathbf{k})\right]\left(2E^{\beta} + E^{\eta}\right)\\ &+ \eta(\mathbf{k})\,E^{\eta} + 2\beta(\mathbf{k})\,E^{\beta}\\ &+ \left[1-2\alpha(\mathbf{k})\right]a_\nu + \frac{1}{4}\left[b_\nu + 2\beta(\mathbf{k})c_\nu + \eta(\mathbf{k})d_\nu\right].\end{aligned} \tag{48}$$

The various parameters appearing above are defined as:

$$C^{\alpha} = \left\langle c^{\alpha}(i)\,c^{\dagger}(i)\right\rangle \tag{49}$$

$$C^{\lambda} = \left\langle c^{\lambda}(i)\,c^{\dagger}(i)\right\rangle \tag{50}$$

$$C^{\varpi} = \left\langle c^{\varpi}(i)\,c^{\dagger}(i)\right\rangle \tag{51}$$

$$D = 1 - \left\langle \xi(i)\,\xi^{\dagger}(i)\right\rangle - 2\left\langle \eta(i)\,\eta^{\dagger}(i)\right\rangle \tag{52}$$

$$E^{\beta} = \left\langle c^{\beta}(i)\,\eta^{\dagger}(i)\right\rangle \tag{53}$$

$$E^{\eta} = \left\langle c^{\eta}(i)\,\eta^{\dagger}(i)\right\rangle \tag{54}$$

$$\begin{aligned}a_\nu = &\,2\left\langle c^{\dagger}(i)\,\sigma_\nu\,c^{\alpha}(i)\,c^{\dagger}(i)\,\sigma_\nu\,c^{\alpha}(i)\right\rangle\\ &- \left\langle c^{\alpha\dagger}(i)\,\sigma_\nu\,\sigma^{\lambda}\,\sigma_\nu\,c^{\alpha}(i)\,n_\lambda(i)\right\rangle\end{aligned} \tag{55}$$

$$\begin{aligned}b_\nu = &\,2\left\langle c^{\dagger}(i)\,\sigma_\nu\,c^{\dagger}(i)\,\sigma_\nu[c(i)\,c(i)]^{\alpha}\right\rangle\\ &- \left\langle c^{\dagger}(i)\,\sigma_\nu\,\sigma^{\lambda}\,\sigma_\nu\,c(i)\,n_\lambda^{\alpha}(i)\right\rangle\end{aligned} \tag{56}$$

$$\begin{aligned}c_\nu = &\,2\left\langle c^{\dagger}(i)\,\sigma_\nu\,c^{\dagger}(i^{\eta})\,\sigma_\nu\,c(i^{\alpha})\,c(i^{\alpha})\right\rangle\\ &- \left\langle c^{\dagger}(i)\,\sigma_\nu\,\sigma^{\lambda}\,\sigma_\nu\,c(i^{\eta})\,n_\lambda(i^{\alpha})\right\rangle\end{aligned} \tag{57}$$

$$\begin{aligned}d_\nu = &\,2\left\langle c^{\dagger}(i)\,\sigma_\nu\,c^{\dagger}(i^{\beta})\,\sigma_\nu\,c(i^{\alpha})\,c(i^{\alpha})\right\rangle\\ &- \left\langle c^{\dagger}(i)\,\sigma_\nu\,\sigma^{\lambda}\,\sigma_\nu\,c(i^{\beta})\,n_\lambda(i^{\alpha})\right\rangle\end{aligned} \tag{58}$$

where we used the notation

$$i = (i_x, i_y, t) \tag{59}$$

$$i^{\alpha} = (i_x + a, i_y, t) \tag{60}$$

$$i^{\eta} = (i_x + 2a, i_y, t) \tag{61}$$

$$i^{\beta} = (i_x + a, i_y + a, t). \tag{62}$$

References

1. R. Coldea, S. Hayden, G. Aeppli, T. Perring, C. Frost, T. Mason, S.-W. Cheong, Z. Fisk, Phys. Rev. Lett. **86**, 5377 (2001)
2. P. Anderson, Vol. 1 (Academic, New York, 1963), p. 25
3. C. Canali, S. Girvin, M. Wallin, Phys. Rev. B **45**, 10131 (1992)
4. R. Singh, M. Gelfand, Phys. Rev. B **52**, 15695 (1995)
5. O. Syljuåsen, H. Rønnow, J. Phys. Cond. Matt. **12**, 405 (2000)
6. H. Rønnow *et al.* (2001), `cond-mat/0101238`
7. M. Takahashi, J. Phys. C. **10**, 1289 (1977)
8. M. Roger, J. Delrieu, Phys. Rev. B **39**, 2299 (1989)
9. A. MacDonald, S. Girvin, D. Yoshioka, Phys. Rev. B **37**, 9753 (1988)
10. C. Peters *et al.*, Phys. Rev. B **37**, 9761 (1988)
11. A. MacDonald, S. Girvin, D. Yoshioka, Phys. Rev. B **41**, 2565 (1990)
12. F. Mancini, S. Marra, H. Matsumoto, Physica C **244**, 49 (1995)
13. F. Mancini, S. Marra, H. Matsumoto, Physica C **250**, 184 (1995)
14. F. Mancini, S. Marra, H. Matsumoto, Physica C **252**, 361 (1995)
15. F. Mancini, D. Villani, H. Matsumoto, Phys. Rev. B **57**, 6145 (1998)
16. A. Avella, F. Mancini, R. Münzner, Phys. Rev. B **63**, 245117 (2001)
17. F. Mancini, V. Turkowski, Acta Phys. Pol. A **101**, 505 (2002)
18. V. Yushankhai, V. Oudovenko, R. Hayn, Phys. Rev. B **55**, 15562 (1997)
19. N. Peres, M. Araújo (2002), `cond-mat/0201151`
20. F. Mancini, S. Marra, A. Allega, H. Matsumoto, in *Superconductivity and Strongly Correlated Electron Systems* (World Scientific, Singapore, 1994), p. 271
21. F. Mancini, A. Avella (2000), `cond-mat/0006377`